Dielectric properties of TiC_x, TiN_x, VC_x, and VN_x from 1.5 to 40 eV determined by electron-energy-loss spectroscopy

J. Pflüger,* J. Fink, W. Weber, and K.-P. Bohnen
Institut für Nukleare Festkörperphysik, Kernforschungszentrum Karlsruhe GmbH, Postfach 3640, D-7500 Karlsruhe, Federal Republic of Germany

G. Crecelius
Institut für Festkörperforschung, Kernforschungsanlage Jülich, Postfach 1913, D-5170 Jülich 1, Federal Republic of Germany
(Received 21 February 1984)

The optical properties of TiC_x, TiN_x, VC_x, and VN_x in the energy range 1.5 to 40 eV were determined with the use of electron-energy-loss spectroscopy. The optical joint density of states deduced from a Kramers-Kronig analysis were compared with joint densities of states calculated from self-consistent Gaussian-LCAO band-structure data. Good agreement between theory and experiment was obtained. Characteristic differences among the spectra of the particular compounds are discussed in terms of different electronic properties deduced from band-structure calculations. The influence of nonmetal vacancies on the optical properties was investigated.

I. INTRODUCTION

The $3d$—transition-metal nitrides and carbides (TMNC's) belong to the group of refractory compounds.[1,2] They show metallic as well as covalent and ionic properties, which make them interesting for both technical applications and fundamental research. Their great hardness and brittleness and their high melting points are typical for compounds with strong covalent bonds. Metallic properties are their electrical conductivity, superconductivity, and their metallic color. Many TMCN's such as TiC, TiN, VC, and VN crystallize in the cubic NaCl structure which is typical for ionic crystals. Another interesting property of the TMNC's is their tendency to form vacancies on the nonmetal sites. For example, TiC_x exists in the NaCl phase for $0.53 \leq x \leq 1.0$.[2] For some compounds such as VC it is impossible to obtain a nonmetal-to-metal ratio close to one without the presence of free carbon.

The unusual physical properties are closely related to the electronic structure. Experimentally electronic properties have been investigated with use of x-ray-induced photoelectron spectroscopy[3,4] (XPS), ultraviolet-photoelectron spectroscopy[5–9], x-ray emission,[10–15] bremsstrahlung-isochromat spectroscopy,[16] and electron-energy-loss spectroscopy (ELS) in reflection[8,9] as well as in transmission.[17] A number of optical reflectivity measurements have also been published.[18–25]

On the theoretical side, the first energy-band calculations have been carried out by Bilz in 1958.[26] Since then, numerous band-structure calculations have been performed (for reviews see Calais[27] and Neckel[28]). The most comprehensive work on this field was done by Neckel and collaborators,[29–33] who in particular presented a systematic study on a number of $3d$—transition-metal carbides, nitrides, and oxides using a self-consistent augmented-plane-wave method.[29] In these calculations the close similarity of all TMNC compounds as well as some systematic trends in their electronic structure become evident. These features are visualized in a comparison of the partial electronic densities of states of the Ti and V carbides, nitrides, and oxides shown in Fig. 1. The nonmetal s orbitals form the lowest valence band. On going from the carbides to the oxides, it separates more and more from the other valence bands. Next is a set of three bands formed mainly from nonmetal p orbitals. However, there is a strong hybridization with metal d orbitals in these bands, which is the origin of the strong covalent bonding of the TMNC's. This d admixture is decreasing from the carbides to the oxides. The next five bands consist mainly of metal d orbitals with some admixture of p orbitals. Again, the p character in the d bands is stronger in the carbides than in the oxides or nitrides. With respect to the p-d hybridization, these upper bands form the antibonding states while the lower p bands form the bonding states. The position of the Fermi energy (E_F) is determined by the number of available valence electrons. In the case of TiC, E_F is situated in the very minimum of the density of states (DOS). With an increasing number of valence electrons E_F is shifted upward into the d bands and the DOS at E_F increases. We note that all states made up of metal $4s$ orbitals are shifted far above the Fermi level. This is caused by the hybridization with the nonmetal s orbitals.

During the past few years the effects of nonmetal vacancies on the electronic properties of the TMNC's have gained increasing interest. Experimental methods applied were ELS (Ref. 17), reflectivity measurements,[18,19,21–24] and XPS.[34,35] Theoretically tight-binding coherent-potential approximation (TBCPA)[36–38] cluster[39,40] and supercell band-structure calculations[41,42] have been performed. The results of the TBCPA studies differ markedly from those of the other approaches. The latter predict new defect states in the low DOS region below E_F, and thus a downward shift of E_F, while the TBCPA results predict an upward shift in E_F.

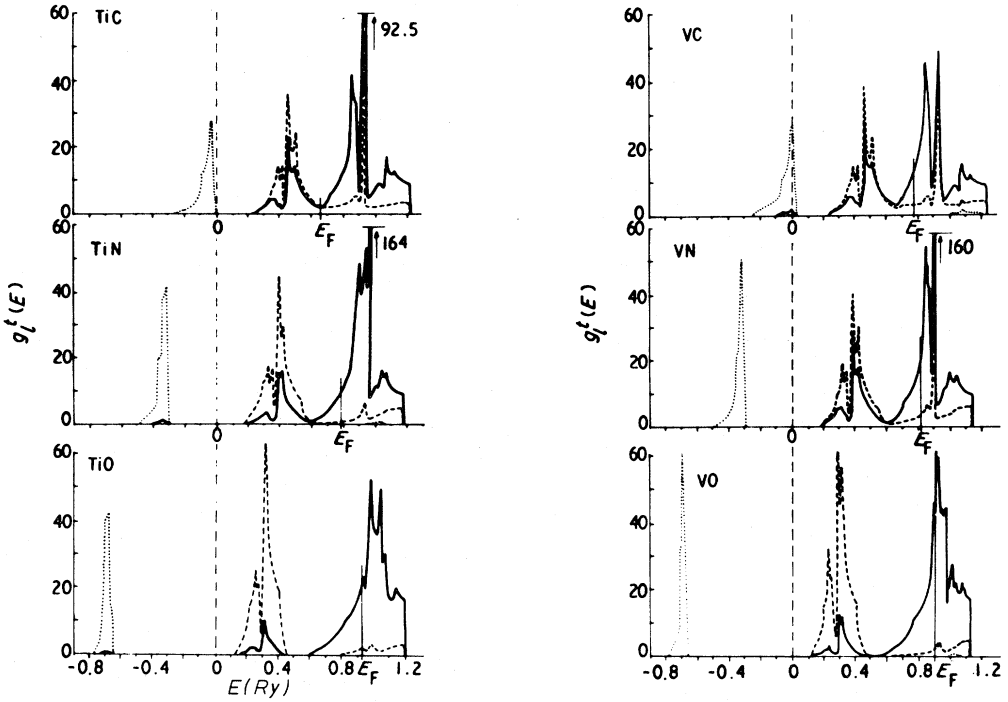

FIG. 1. Partial densities of states of TiC, TiN, TiO, VC, VN, and VO taken from Ref. 28. Dotted lines: nonmetal *s*-like DOS; dashed lines: nonmetal *p*-like DOS; solid lines: metal *d*-like DOS.

ELS using high-energy (170 keV) electrons is a powerful tool to investigate the electronic structure of matter. In contrast to reflection ELS measurements, where electrons of typically 1000 eV are reflected from surfaces as clean as possible, high-energy ELS offers several unique advantages.[43,44] First, only bulk contributions are measured; possible surface contamination with one or even a few monolayers of adsorbed atoms does not influence the results. Reflection ELS measurements are very surface sensitive and volume and surface losses are difficult to separate. It is therefore not possible to determine a pure volume loss function. Second, our measurements are performed with a definite momentum transfer (q) whereas in reflection the scattering of electrons is a two-step process, an elastic scattering event with large q followed by an inelastic scattering event with small q. Thus only the high-energy ELS allows the determination of the loss function $\mathrm{Im}[-1/\epsilon(\vec{q},E)]$ and using a Kramers-Kronig analysis (KKA) the momentum- and energy-dependent dielectric function $\epsilon(\vec{q},E)$ can be evaluated.

If the measurements are performed with vanishing momentum transfer, optical and ELS measurements produce identical results. Yet ELS spectra can easily be extended to energy ranges where optical work is only possible using synchrotron radiation. Because optical as well as ELS data have to be Kramers-Kronig-analyzed in order to extract the dielectric function, the spectra must be measured in an energy range which well exceeds the plasma energy in order to reduce the influence of the extrapolations used in the KKA.

Optical data are important sources of information about electronic properties of matter. They reflect transitions between valence- and conduction-band states and comparisons with band-structure data can be made. In spite of the many existing experimental papers on TMNC's, optical measurements in a large energy range exist only for TiC from 0.1 to 30 eV.[18] For TiN the energy range is much more limited.[20–23] For VC and VN no optical data exist. The aim of this contribution was therefore a systematic study of TiC, TiN, VC, and VN in a large energy range as well as a detailed comparison of experimental results with band-structure data. A point of special interest was the influence of nonmetal vacancies on the electronic properties.

II. EXPERIMENTAL

A. Sample preparation and characterization

The preparation of samples suited for ELS measurements is a crucial problem. They must be self-supporting with a homogeneous thickness of about 50—100 nm and should have an area of several square millimeters.

All samples for this work were prepared by reactive sputtering onto a substrate material that could be dissolved without affecting the sputtered layers. A Perkin-Elmer-Randex 3140 HF-sputtering system was used. The base pressure before sputtering was typically $(2—5)\times10^{-8}$ Torr. For the nitrides an argon/nitrogen atmosphere and for the carbides an argon/methane atmosphere was used. The metal-to-nonmetal ratio of the sputtered films could be varied over a wide range by carefully changing the methane or nitrogen partial pressure, while the HF power and the argon partial pressure were kept constant. Before preparation the target was presputtered for about 60 min in argon and the substrate was degassed at about 1500 °C

for several minutes. The substrate material was $0.015\times100\times25$ mm Molybdenum foil clamped on a Tantalum strip that was heated directly by passing a current of 100—200 A through it. The substrate material was kept at 800—1200 °C during sample preparation. The substrate temperature was measured with a pyrometer. The total pressure with a hot (900 °C) sample holder was typically about 10^{-7} Torr. The sputtered films were floated off in aqueous $FeCl_3$ solution and cleaned in distilled water several times. For the different analysis procedures to be described below the films were supported by sapphire substrates. In addition the nitride films were supported by high-purity carbon substrates for nitrogen analysis. For the ELS measurements the films were supported on standard TEM grids (100—200 mesh). In this way samples with an area of up to 1 cm^2 and a thickness of 400—1200 Å could be prepared.

The film thickness and the nitrogen content of the nitrides were determined by Rutherford backscattering (RBS) of 2.0-MeV α particles.[45] On TiC samples a $^{12}C(d,p)^{13}C$ nuclear reaction with 1.27-MeV deuterons was used[46] to obtain [C]/[Ti] ratios with an accuracy of about $\pm10\%$. With the RBS measurements on carbon-supported nitride films, a possible oxygen contamination could be detected. In the RBS spectra of all samples no traces of Mo, Fe, and Cl could be observed. The carbon contents of the VC samples were deduced from lattice parameters only.[2] A relative [C]/[V] scale was obtained from ELS measurements of the carbon K- and vanadium $L_{2,3}$-absorption-edge spectra. An energy-dependent background was subtracted and the spectra were integrated up to 50 eV above the edge. The ratio of these areas is proportional to the [C]/[V] ratio.[47] An oxygen analysis in the carbide samples was not possible because sapphire substrates (Al_2O_3) were used. But no oxygen could be detected in the ELS spectra at energy losses corresponding to the binding energy of the oxygen K edge.

The lattice parameters were determined with a thin-film Seemann-Bohlin-diffractometer/camera. With this technique lattice parameters could be measured even at 400-Å films with an average error of several 10^{-3} Å. Also a possible contamination with phases other than fcc could be excluded. For the measurements only single-phase samples with the pure NaCl phase were used. For TiC the lattice parameters as a function of carbon content agreed within error bars with data given by Storms.[2] Also, the relatively large lattice parameters are strong hints for only minor oxygen contaminations because in TiC oxygen tends to reduce the lattice parameters.[2]

For the TiN and VN samples an additional check of sample quality was obtained by measuring the superconducting transition temperature (T_c) with an inductive method. TiN and VN have T_c's of 5.5 and 8.5 K, respectively, while TiC and VC have T_c's below 1.2 K.[1] In the nitrides T_c is a very sensitive measure of oxygen content and vacancy concentration.[1] For comparison we have also investigated TiN films prepared by chemical vapor deposition which had a T_c of about 5.4 K (Ref. 48) with no further information available. The measurements performed with this sample were in good agreement with those of the sputtered films. In Table I a summary of the properties of all samples used in this work is given.

B. Spectrometer

The ELS measurements have been performed with a spectrometer using monochromatized electrons with a kinetic energy of 170 keV. Monochromator and analyzer are on high potential while the sample is kept on earth potential. Thus the sample can be manipulated easily. Electrostatic hemispherical deflectors according to the Kuyatt-Simpson design were used as monochromator and analyzer.[49] With the help of a zoom-lens electron optic between monochromator (analyzer) and accelerator it was possible to vary the angular spread of the primary electrons (momentum resolution), while the energy resolution could be changed with the pass energy of the electrons. Thus an energy resolution $0.09\leq\Delta E\leq0.4$ eV and a momentum resolution $0.03\leq\Delta q\leq0.2$ Å^{-1} could be selected. Beam currents up to 200 nA can be transmitted through the spectrometer for $\Delta E\cong0.4$ eV and $\Delta q\cong0.2$ Å^{-1}. For the measurements of this work the energy reso-

TABLE I. Properties of the samples used in this work.

Sample	Metal/nonmetal ratio	lattice constant (Å)	Transition temperature (K)	Thickness (Å)
TiC 50	0.7±10%	4.323±0.001		1100
TiC 31	1.0±10%	4.334±0.003		770
VC 104	0.78[a]	4.15 ±0.1		620
VC 103	0.88[a]	4.172±0.003		590
TiN 88	0.9±5%	4.238±0.004	<1.2	950
TiN 92	0.95[b]	4.245±0.002	3.1	1300
TiN 45[c]	1.0±5%	4.25	4.6—5.6	460
TiN CVD[d]			5.4	
VN 9[c]	1.0±5%	4.134	7.9—8.1	450
VN 10	0.82±5%	4.10 ±0.01	5.7	870

[a]Determined from lattice parameter measurements and values given by Ref. 2.
[b]Determined from transition temperature and Ref. 1.
[c]Spectra from stoichiometric TiN and VN were recorded from several samples. Typical values are given.
[d]Prepared by chemical vapor deposition (see Ref. 48).

lution was fixed at 0.1 eV and two momentum resolutions of $\Delta q=0.04$ and 0.08 Å^{-1} were used. The maximum transmitted currents were 1 and 4 nA, respectively.

C. Evaluation of the optical constants

A high-energy ELS experiment consists in irradiating a sample about 1000 Å thick, with a beam of monochromatic electrons ($E_0=170$ keV; $\Delta E=0.1$ eV). The current transmitted through the sample is measured as a function of energy and escape angle. Surface losses as well as volume losses contribute to the measured spectrum.[43,44,50] However, the intensity of surface losses rapidly decreases with increasing momentum transfer q. Therefore, a q of 0.1 Å^{-1} is sufficiently large to suppress surface losses almost completely but is small when compared to the dimensions of the Brillouin zone (typically 1.5 Å^{-1} for the TMNC's). In order to evaluate the dielectric properties we closely followed the procedure described by Daniels *et al.*:[50] The elastic line was removed by a linear extrapolation of the loss spectrum between 0 and 1.2 eV. The spectrum was then deconvoluted to account for finite energy and momentum resolution of the spectrometer. For this step the momentum distribution was recorded before each measurement. Our spectrometer has a momentum resolution of about 0.04–0.08 Å^{-1} so that the correction of the deconvolution procedure to the measured spectrum was typically smaller than 10%. Also, the same algorithm as described in Ref. 50 was used to correct for double scattering. After this step a spectrum was obtained which is proportional to the volume loss function $\mathrm{Im}(-1/\epsilon)$. Real and imaginary parts of $1/\epsilon$ are connected via the Kramers-Kronig relations. To obtain the real part of $1/\epsilon$, a Kramers-Kronig transformation was performed numerically. For energies larger than 40 eV, the spectrum was extrapolated proportionally to E^{-3}, which is the loss function of a free-electron gas. For a metal $\mathrm{Re}(1/\epsilon)$ is equal to zero at $E=0$. This condition was used to determine the proportionality constant of the loss function. Once real and imaginary parts of $1/\epsilon$ were known, the dielectric function, optical joint density of states, reflectivity, etc., could be calculated.

In Fig. 2 our results for TiC are compared to the optical data of Ref. 18. The results derived with the two methods agree quite satisfactorily.

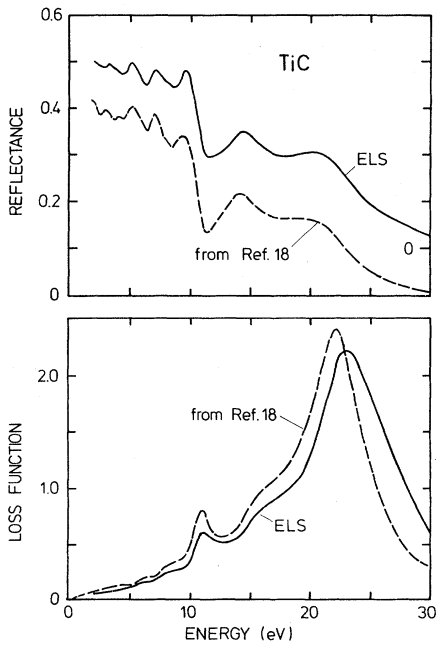

FIG. 2. Comparison of optical and ELS results. Upper part: measured reflectivity of Ref. 18 versus reflectivity calculated from the ELS results of this work. Lower part: measured loss function versus curve as calculated from reflectivity data of Ref. 18.

III. RESULTS

A. Stoichiometric compounds

The loss functions and the real and imaginary parts of the dielectric function derived by a Kramers-Kronig analysis for $TiC_{1.0}$, $TiN_{1.0}$, $VC_{0.88}$, and $VN_{1.0}$ are shown in Figs. 3(a)–3(d). We note that it is impossible to prepare VC_x for x larger than 0.88.

Comparing the loss functions with the ϵ_1 and ϵ_2 curves, a maximum in $\mathrm{Im}(-1/\epsilon)$ corresponds to a zero or at least a small absolute value of ϵ_1 and a small ϵ_2. The better this condition is fulfilled the more pronounced is the maximum in the loss function.

The dominant feature in all loss spectra is the volume plasmon at 23.5, 24.9, 24.9, and 26.3 eV for TiC, TiN, VC, and VN, respectively. We may compare these values to the corresponding free-electron plasma energies calculated from

$$E_p=\hbar\left[\frac{4\pi e^2 N}{mV_a}\right]^{1/2}. \tag{1}$$

(e is the elementary charge, m is the free-electron mass, N the number of valence electrons per unit cell, and V_a is the unit-cell volume.) As valence orbitals we consider the metal $3d$ and $4s$ orbitals and nonmetal $2s$ and $2p$ orbitals. We obtain 23.3, 25.5, and 28.0 eV calculated for $TiC_{1.0}$, $TiN_{1.0}$, $VC_{0.88}$, and $VN_{1.0}$. Other values found in the literature are 22.6 eV for $TiC_{0.9}$ (Ref. 18) and 25.3 eV for VN.[8]

Apart from the main plasmon peak, the spectra of TiC and VC are very similar to each other, and the same holds for the TiN and VN spectra. Yet there are considerable differences between the spectra of the carbides and those of the nitrides. One is the presence of the low-energy plasmon in the nitrides (very sharp at 2.8 eV in TiN, and somewhat broadened at 3.2 eV in VN), which is not seen in the carbides. Some authors[8,9] have claimed that this feature is common to all TMNC's, yet our data clearly show that this is not the case.

We now present a simple Drude-Lorentz model for the formation of the low-energy plasmon loss[51,52] [see Figs. 4(a)–4(c)]. One fraction of the total valence-electron concentration is assumed to be free. We assumed one conduction electron to behave similar to a free electron (this is about the Drude electron concentration in TiN). A strong oscillator, caused by interband transitions of four valence electrons, is placed at $E_B=7$ eV, representing a

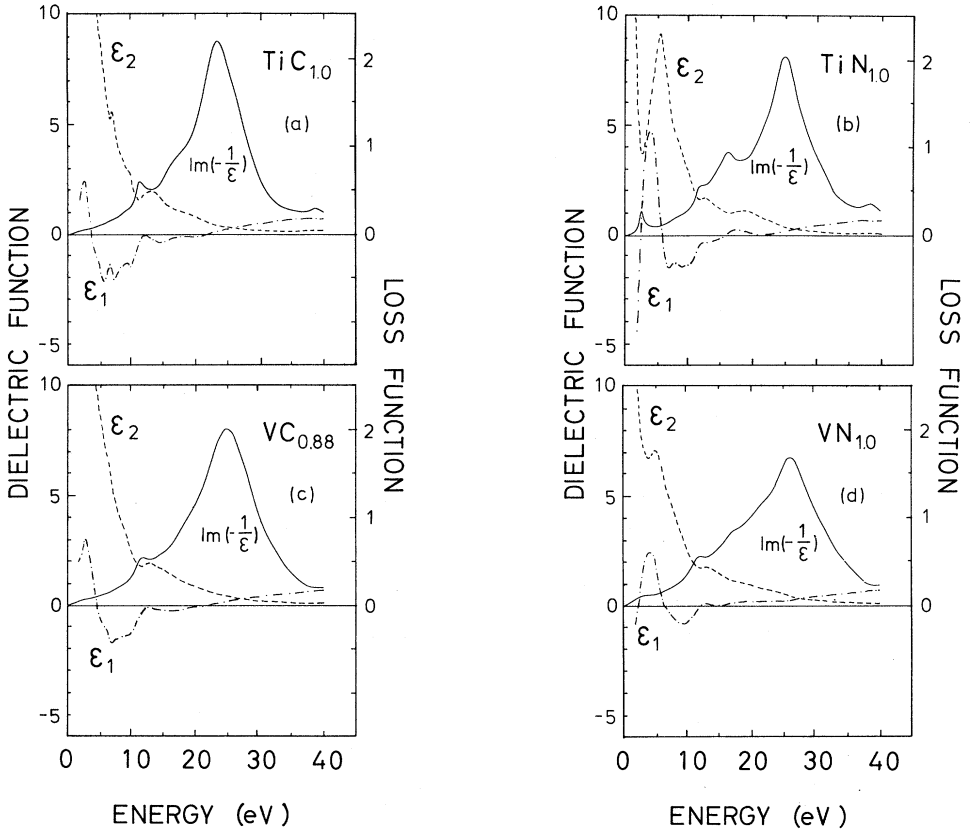

FIG. 3. Loss functions (solid lines) and Kramers-Kronig—derived real and imaginary parts of the dielectric function ϵ_1, ϵ_2 (dotted-dashed and dashed lines).

strong interband transition at this energy (see also next section). Figure 4(a) shows the Drude contributions to ϵ_1 and ϵ_2 for two different damping constants Γ_0 (dotted-dashed lines correspond to $\Gamma_0=1.5$ eV, solid lines to $\Gamma_0=3.0$ eV). The resulting loss function is also shown. The contribution of the pure interband transitions on ϵ_1 and ϵ_2 and the corresponding loss function are shown in Fig. 4(b). Figure 4(c) shows the ϵ_1 and ϵ_2 curves and the loss function when the Drude and interband contribution to the dielectric function are added. The similarity of $\mathrm{Im}(-1/\epsilon)$ to the measured spectra is evident. Owing to the large positive value of ϵ_1 of the interband contribution, the zero in ϵ_1 is shifted down to about 2.8 eV. The resulting loss function has a maximum (plasmon) at this value. Assuming that the oscillator strength of the interband transitions is exhausted, the upper peak of the loss function corresponds roughly to a plasmon due to five electrons. An increase of the Drude damping constant in Fig. 4(c) (solid lines) leads to a filling of the minimum in ϵ_2 and a damping of the resulting plasmon. A further enhancement of ϵ_2 (e.g., an additional oscillator) in the minimum would completely damp out the plasmon as we observe in TiC. Thus with this simple picture we can argue that only weak absorption at energies up to 3 eV is present in TiN. Absorption is considerably stronger in VN but even stronger in the carbides so that the Drude plasmon is damped out. This conclusion is fully consistent with reflectivity data. In TiN (Refs. 20, 21, and 23) the reflectivity up to 2.5 eV is quite high and only minor absorption occurs. In TiC strong absorption can be observed even at very low energies.[18] The other structures in the spectra are caused by additional interband transitions and will be discussed in detail in the next section.

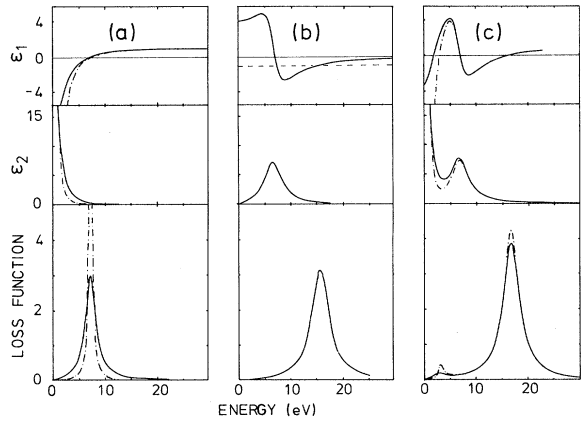

FIG. 4. Formation of the low-energy plasma excitation in TiN and VN. For details see text.

At 38.5 eV the onset of the Ti $3p$ core excitation is visible in the TiC and TiN spectra. The corresponding transition for the vanadium compounds was out of the range of measured energies. Because at higher energies the polarizability of the medium becomes rather small, $\epsilon_1 \cong 1$ and $\epsilon_2 \ll 1$, and thus the loss function is proportional to ϵ_2.

B. Optical joint densities of states

The optical joint density of states (OJDS) is defined as[53]

$$J_1(E)=\frac{E\epsilon_2(E)}{\frac{1}{2}\pi E_p^2}\ , \tag{2}$$

where E_p is defined by Eq. (1). Within the random-phase approximation and neglecting local-field effects this quantity may be written as

$$J_1(E)=\frac{2}{\pi E_p^2}\left[\frac{E_{p0}^2\Gamma_0}{E^2+\Gamma_0^2}+\sum_{\substack{n,n',\vec{k}\\ n\neq n'}} f_{n,n',k}\,\delta(E_{n',k}-E_{n,k}-E)\right], \tag{3}$$

and E_{p0} is the Drude plasma energy, Γ_0 is an empirical damping constant to account for defect scattering, and $f_{n,n',k}$ is the oscillator strength for a transition from an occupied state in band n and wave vector k to an unoccupied state in band n' with the same wave vector. The summation goes over all occupied bands n, all unoccupied bands n', and over all $\vec{k}$ points in the first Brillouin zone. The δ function represents energy conservation. The first term is usually called the Drude (or intraband) contribution, the second is the interband contribution. The intraband contribution arises from transitions between occupied and unoccupied states at the Fermi surface which are broadened by finite lifetime effects. It is easily seen in Eq. (3) that the transition energies as well as their strengths enter directly in the OJDS. If all interband transitions occur at energies which are larger than the Drude damping constant Γ_0, intraband and interband contributions to the OJDS can easily be separated. This is the case in a number of transition metals[50] and will also be of some importance in the discussion below.

In the simplest approximation we assume the oscillator strengths $f_{n,n',k}$ to be constant. Then the OJDS is proportional to the joint density of states[53] (JDS) which is defined as

$$J_0(E)=\sum_{\substack{n,n',\vec{k}\\ n\neq n'}}\delta(E_{n',k}-E_{n,k}-E)\ . \tag{4}$$

This function can be calculated if the energy bands are known. We have calculated the energy bands of stoichiometric TiC, TiN, VC, and VN with the self-consistent Gaussian-LCAO method of Appelbaum and Hamann.[54] A large set of basis functions was necessary to obtain reliable energy bands even at energies well above the Fermi level. The total densities of states calculated from these bands were in excellent agreement with those given by Neckel *et al.*[29] The optical joint densities of states were calculated using the tetrahedral method[55] on a 89-point mesh in the irreducible part of the Brillouin zone.

In Figs. 5(a)—5(d) the OJDS which were determined by the Kramers-Kronig analysis are shown by the solid lines. The JDS functions calculated from the band-structure data are shown by the dashed lines.

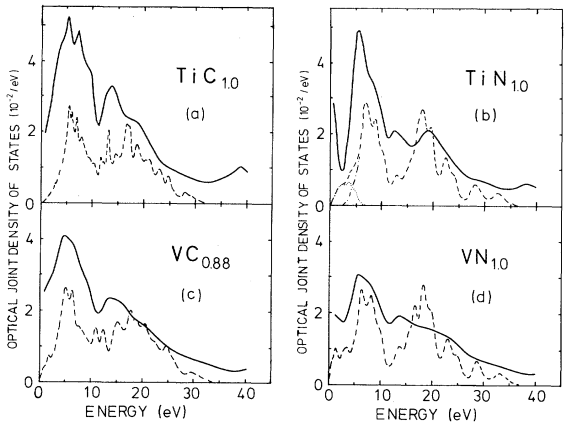

FIG. 5. Kramers-Kronig—derived optical joint densities of states of the stoichiometric compounds (solid lines) and joint densities of states from our band-structure calculations (dashed lines). In the TiN curves, the joint density of states for transitions between d bands and without d-d transitions are shown separately (dotted and dotted dashed lines, respectively).

Common to all spectra is a broad maximum centered at 5—7 eV. Otherwise, carbide and nitride spectra look quite different. One characteristic difference is a pronounced minimum in the OJDS at 2.8 eV in TiN and a shallow one at 3.2 eV in VN: They are closely related to the plasma losses observed at these energies. The carbides show a continuous increase of OJDS up to 7 eV. It is dominated by intraband transitions up to several eV. This is readily seen in TiN where intraband and interband contributions are energetically well separated. The Drude parameters E_{p0} and Γ_0 can than be found by fitting the first term of Eq. (3) to the spectrum up to about 2.5 eV. The values thus obtained are $E_{p0}=8.1$ eV and $\Gamma_0=1.1$ eV. These values agree well with others for E_{p0} and Γ_0 found in the literature.[20–33]

In VN intraband and interband contributions mix more strongly so that we did not try to determine the Drude parameters. In the carbides the mixing is so strong that both contributions cannot be observed separately.

The physical reasons for the differences observed in the four compounds may be understood with the help of the partial densities of states of Ref. 29 (see Fig. 1). An equivalent explanation of the optical properties of titanium carbonitrides was given by Karlsson *et al.*[23] In TiN the Fermi level lies within the d bands and the states around E_F are almost pure metal d states with only a very weak nonmetal p character. In VN the situation is similar except that the nonmetal p-like DOS is several times larger than in TiN although still small compared to the d component. In TiN optical transitions between states made up purely of metal d orbitals are dipole-forbidden in the on-site approximation. Thus interband absorption sets in when (intersite) transitions from the occupied p bands to unoccupied d bands become possible. To underline this we calculated the JDS for d-d transitions in TiN [see Fig. 5(c), dotted curve]. The JDS without these d-d transitions was also calculated [dotted-dashed curve in Fig. 5(c)]. It

starts at about 2.8 eV when transitions from p to d bands become possible. Thus the intraband contribution is not affected by interband transitions up to this energy. In VN, the interband contribution has increased so that the damping of the Drude plasmon oscillation is stronger. This is seen in the loss function as well as in the OJDS. As in TiC, E_F is situated in the minimum of the DOS between p and d bands, p-d transitions are possible at all energies so that interband absorption can always occur. Intraband and interband contributions therefore mix strongly. Some care must be taken in the interpretations of the VC spectrum because of the influence of nonmetal vacancies on the optical properties. We note that we have already measured stoichiometric NbC, ZrN, and NbN which are isoelectronic to VC, TiN, and VN, respectively. They all showed a similar behavior to TiN and VN, i.e., a low-energy plasma loss and a corresponding dip in the OJDS.[56]

Structures above 3 eV are only affected by interband transitions. The broad hump at 5—7 eV corresponds to p-d transitions. Its initial rise is shifted according to the position of E_F. In TiC it starts earlier than in TiN, VC, and VN. Furthermore, the structure in TiC is subdivided into two peaks and a shoulder which can be attributed to transitions between maxima in the DOS in the occupied p and unoccupied d bands. In the other compounds, these structures are less pronounced. Maxima in the carbide spectra above 10 eV can be attributed to transitions from C 2s states to unoccupied states in the d bands. In the nitride spectra the corresponding transitions start at about 19 eV. Therefore, the maximum around 12 eV must be attributed to transitions between the (nonmetal) p bands and to the (metal) s-p bands above the d bands.

The qualitative interpretation as obtained from an inspection of the energy bands and the corresponding DOS curves is confirmed by a calculation of the JDS [see Figs. 5(a)—5(d)]. Peaks and shoulders up to roughly 10 eV are reproduced quite well by the theoretical curve. Because lifetime effects were neglected, the JDS show more structure than is actually present. Also, due to matrix-element effects intensities are not reproduced correctly.

Again, in the titanium compounds the onset of the Ti 3p core excitation is visible at 38.5 eV. This was also seen in the corresponding loss functions.

C. Influence of stoichiometry

The loss functions of the substoichiometric compounds are shown in Fig. 6. In comparison with the loss functions shown in Figs. 3(a)—3(d), some differences are evident. The positions of the main volume plasmon is shifted down from 23.5, 24.9, 24.9, and 26.3 eV in the stoichiometric case to 23.2, 24.6, 24.6, and 25.9 eV for $TiC_{0.7}$, $TiN_{0.9}$, $VC_{0.8}$, and $VN_{0.82}$, respectively. However, this shift to lower energies is less than one would expect from the nominal decrease of the valence-electron concentration due to nonmetal vacancies and from the application of Eq. (1). In addition, sharp and pronounced structures of the stoichiometric compounds become broad and washed out if vacancies are present. This is best seen by a comparison of the $TiC_{1.0}$ spectrum in Fig. 3(a) and the

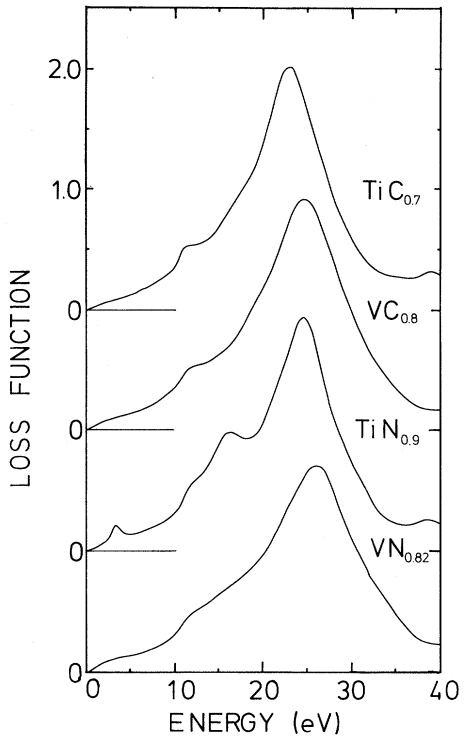

FIG. 6. Loss functions of the substoichiometric compounds $TiC_{0.7}$, $VC_{0.8}$, $TiN_{0.9}$, and $VN_{0.82}$.

$TiC_{0.7}$ spectrum in Fig. 6.

The low-energy plasma excitation at 2.8 eV in $TiN_{1.0}$ has shifted up to 3.3 eV in $TiN_{0.9}$. In addition, its width has increased considerably. In $VN_{0.82}$ this peak is so much broadened that it cannot be distinguished from the background. This is a further indication that the observed $VC_{0.88}$ spectrum [shown in Fig. 3(c)] is influenced by vacancy effects.

The peaks and structures around 12.5 eV in the carbides and between 12 and 19 eV in the nitrides remain at about the same energies. However, in the $VN_{0.82}$ spectrum it is almost impossible to determine their exact positions.

The Kramers-Kronig—derived OJDS are shown in Fig. 7. The zero of the vertical axis of each curve is shifted as indicated. As was the case with the loss functions, these curves are smeared out and broadened compared to the corresponding spectra of stoichiometric compounds, but the overall shapes are conserved and the similarity with the stoichiometric spectra of Figs. 5(a)—5(d) is still visible. Compared to the stoichiometric compound transitions around 12 eV in the carbides and 19 eV in the nitrides originating from nonmetal 2s states and those around 5—7 eV in all spectra originating from nonmetal 2p states are somewhat reduced. This is due to the fact that fewer nonmetal initial states are available. In the $TiN_{0.9}$ spectrum the minimum in the OJDS has been shifted up to 3.3 eV. This can be understood in the simple Drude-Lorentz model used in the discussion of Fig. 4 (see Sec. III A). In TiN the Drude plasma energy remains independent of stoichiometry. This was found by Rivory *et al.*[21] and is also consistent with our results. However, the damping constant Γ_0 is increased as more defects act as scattering

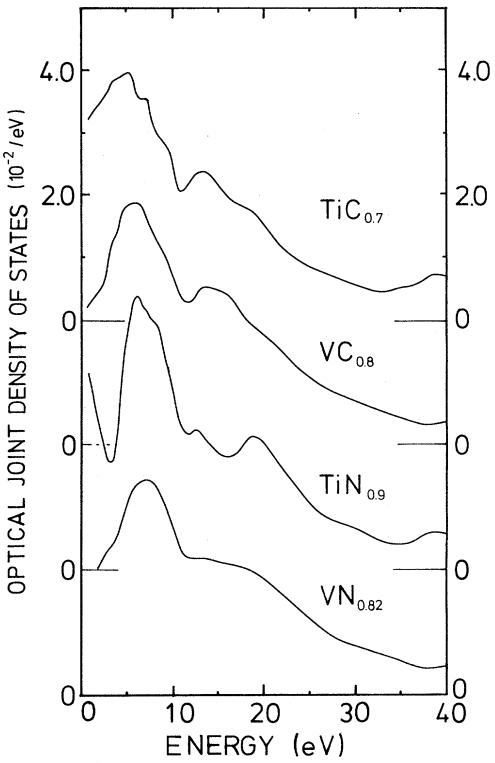

FIG. 7. Kramers-Kronig–derived optical joint densities of states of the loss functions shown in Fig. 6.

centers. This leads to a shallower minimum in the OJDS and to a stronger damping of the plasmon found at this energy. In addition the total oscillator strength for *p-d* transitions is reduced because fewer *p*-like initial states are present. This causes an upward shift of the minimum in the OJDS or alternatively the ϵ_1 of the oscillator in Fig. 4(b) around 3 eV is less positive than in stoichiometric TiN, so that the zero in ϵ_1 corresponding to Fig. 4(c) is found at a somewhat higher energy. Thus the upward shift of the plasmon from 2.8 to 3.3 eV as well as the corresponding minimum in the OJDS is a direct consequence of the reduction of *p*-like initial states and thus of nonmetal vacancies.

The OJDS below 2 eV is larger than in the stoichiometric compounds. An explanation may be that new defect states around the Fermi energy are created as vacancies are present.[39–42] These defects states may allow new transitions which would result in an enhanced transition probability at low energies but also provide an additional damping mechanism for the Drude plasma excitation.

In this point a discrepancy exists between our results and those of Lynch *et al.*[18] There the optical conductivities of $TiC_{0.9}$ and $TiC_{0.64}$ single crystals show only minor differences up to about 4 eV. At present, we have no explanation for this discrepancy; it might be due to different sample's preparation.

IV. SUMMARY

A systematic investigation of the dielectric properties of TiC, TiN, VC, and VN in the energy range from 1.5 to 40 eV was performed using high-energy electron-energy-loss spectroscopy. The samples were prepared by reactive sputtering and carefully analyzed by means of ion-beam techniques, x-ray diffraction, and transmission electron microscopy.

The loss functions of all compounds showed a main maximum near the free-electron plasma energy. Aside from this characteristic differences between carbides and nitrides were observed. A low-energy plasma loss in the nitride spectra was observed which was shown to be the Drude plasma excitation shifted down by strong interband transitions at higher energies. In the carbides this plasma loss was damped out by low-energy interband transitions which become dipole forbidden in the nitrides. Other differences between 12 and 17 eV were also observed.

The OJDS obtained by a Kramers-Kronig analysis were compared to the JDS calculated from self-consistent Gaussian-LCAO band-structure data. While the transition probabilities were dominated by intraband transitions up to roughly 2–3 eV, interband transitions give the dominant contribution for higher energies.

Good agreement between experimental data and the JDS was observed up to 12 eV. Because lifetime effects as well as transition matrix elements are not included in the JDS, these curves predict more structure at higher energies than is seen experimentally and do not reproduce intensities correctly.

We also studied the influence of nonmetal vacancies on the optical quantities. They have four major consequences. First, because the valence-electron concentration is reduced in substoichiometric compounds, the main volume plasmon is slightly shifted down to lower energies. Second, transitions from initial states that have mainly nonmetal character are attenuated. This is observed in all spectra. The reduced oscillator strength of *p-d* transitions is also responsible for the shift of the low-energy plasma excitation from 2.8 to 3.3 eV in going from $TiN_{1.0}$ to $TiN_{0.9}$. Third, because of the increased vacancy concentration, the lifetimes of excited states are reduced because of enhanced scattering on defects. This is not only seen in a general broadening of the structures of the spectra but also in an increased dc conductivity and a larger Drude damping constant Γ_0, especially in TiN_x. Fourth, the OJDS of the substoichiometric compounds at low energies are larger than those of stoichiometric ones. This observation is in qualitative agreement with a number of theoretical papers dealing with the electronic properties of substoichiometric refractory compounds. They predict new states to occur below E_F which lead to new transitions at low energies.

ACKNOWLEDGMENTS

The authors would like to thank R. von Baltz for helpful discussions and W. Schmatz and M. Campagna for continued support. We are indebted to G. Linker, R. Kaufmann, and F. Wüchner for carrying out some of the Rutherford-backscattering measurements.

*Present address: Institut für Festkörperforschung, Kernforschungsanlage Jülich, Postfach 1913, D-5170 Jülich, Federal Republic of Germany.

[1]L. E. Toth, *The Transition Metal Carbides and Nitrides* (Academic, New York, 1971).
[2]E. K. Storms, *The Refractory Carbides* (Academic, New York, 1967).
[3]L. Ramquist, K. Hamrin, G. Johansson, A. Fahlman, and C. Nordling, J. Phys. Chem. Solids **30**, 1835 (1969).
[4]L. I. Johansson, A. L. Hagström, B. E. Jakobson, and S. B. M. Hagström, J. Electron Spectrosc. Relat. Phenom. **10**, 259 (1977).
[5]L. I. Johansson, P. M. Stefan, M. L. Shek, and A. N. Christensen, Phys. Rev. B **22**, 1032 (1980).
[6]A. L. Hagström, L. I. Johansson, S. B. M. Hagström, and A. N. Christensen, J. Electron Spectrosc. Relat. Phenom. **11**, 75 (1977).
[7]J. H. Wheaver and F. A. Schmidt, Phys. Lett. **77A**, 73 (1980).
[8]W. K. Schubert, R. N. Shelton, and E. L. Wolf, Phys. Rev. B **23**, 5097 (1981).
[9]W. K. Schubert, R. N. Shelton, and E. L. Wolf, Phys. Rev. B **24**, 6278 (1981).
[10]L. Ramquist, B. Ekstig, E. Källne, E. Noreland, and R. Manne, J. Phys. Chem. Solids **30**, 1849 (1969).
[11]L. Ramquist, B. Ekstig, E. Källne, E. Noreland, and R. Manne, J. Phys. Chem. Solids **32**, 149 (1971).
[12]D. W. Fischer, J. Appl. Phys. **40**, 4151 (1968).
[13]D. W. Fischer, J. Appl. Phys. **39**, 4757 (1968).
[14]J. E. Holliday, J. Appl. Phys. **38**, 4720 (1967).
[15]V. A. Gubanov, E. Z. Kurmaev, and G. P. Shveikin, J. Phys. Chem. Solids **38**, 201 (1977).
[16]F. Riehle, Th. Wolf, and C. Politis, Z. Phys. B **47**, 3 (1982); **47**, 201 (1982).
[17]J. Pflüger, J. Fink, G. Crecelius, K.-P. Bohnen, and H. Winter, Solid State Commun. **44**, 489 (1982); J. Pflüger, Ph.D. thesis, University of Karlsruhe, 1983, available as Kernforschungszentrum Karlsruhe Report No. KfK-3585, 1983 (unpublished).
[18]D. W. Lynch, C. G. Olson, D. J. Peterman, and J. H. Wheaver, Phys. Rev. B **22**, 3991 (1980).
[19]R. Lye and E. M. Logothetis, Phys. Rev. **147**, 622 (1966).
[20]A. Schlegel, P. Wachter, J. J. Nickl, and H. Lingg, J. Phys. C **10**, 4889 (1977).
[21]J. Rivory, J. M. Behaghel, S. Berthier, and J. Lafait, Thin Solid Films **78**, 161 (1981).
[22]G. Böhm and H. Goretzki, J. Less-Common Met. **27**, 311 (1972).
[23]B. Karlsson, J.-E. Sundgren, and B.-O. Johansson, Thin Solid Films **87**, 181 (1982).
[24]F. W. Fluck, H. P. Geserich, and C. Politis, Phys. Status Solidi **112**, 193 (1982).
[25]J. F. Alward, C. Y. Fong, M. El-Batanouny, and F. Wooten, Phys. Rev. B **12**, 1105 (1975).
[26]H. Bilz, Z. Phys. **153**, 338 (1958).
[27]J. L. Calais, Adv. Phys. **26**, 847 (1977).
[28]A. Neckel, Int. J. Quantum Chem. **23**, 1317 (1983).
[29]A. Neckel, P. Rastl, R. Eibler, P. Weinberger, and K. Schwarz, J. Phys. C **9**, 579 (1976).
[30]A. Neckel, K. Schwarz, R. Eibler, P. Weinberger, and P. Rastl, Ber. Bunsenges. Phys. Chem. **79**, 1053 (1975).
[31]A. Neckel, K. Schwarz, R. Eibler, P. Rastl, and P. Weinberger, Mikrochim. Acta Suppl. 6, 257 (1975).
[32]K. Schwarz and A. Neckel, Ber. Bunsenges. Phys. Chem. **79**, 1071 (1975).
[33]R. Eibler, M. Dorrer, and A. Neckel, J. Phys. C **16**, 3137 (1983).
[34]H. Höchst, P. Steiner, and S. Hüfner, Z. Phys. B **37**, 27 (1980).
[35]H. Höchst, R. D. Bringans, P. Steiner, and Th. Wolf, Phys. Rev. B **25**, 7183 (1982).
[36]J. Klima, J. Phys. C **12**, 3691 (1979).
[37]J. Klima, Czech. J. Phys. B **30**, 905 (1980).
[38]B. M. Klein, D. A. Papaconstantopoulos, and L. L. Boyer, Phys. Rev. B **22**, 1946 (1982).
[39]K. Schwarz and N. Rösch, J. Phys. C **9**, L433 (1976).
[40]G. Ries and H. Winter, J. Phys. F **10**, 1 (1979).
[41]K.-P. Bohnen, W. Weber, and D. R. Hamann, in Kernforschungszentrum Karlsruhe Report No. KfK-3051, 1980 (unpublished).
[42]E. Wimmer, K. Schwarz, R. Podloucky, P. Herzig, and A. Neckel, J. Phys. Chem. Solids **43**, 439 (1982).
[43]R. H. Ritchie, Phys. Rev. **106**, 874 (1954).
[44]H. Raether, in *Solid State Excitations by Electrons,* Vol. 38 of *Springer Tracts in Modern Physics,* edited by G. Höhler and E. A. Niekisch (Springer, New York, 1965), p. 84.
[45]G. Foti, J. W. Mayer, and E. Rimini, in *Ion Beam Handbook for Material Analysis,* edited by J. W. Mayer and E. Rimini (Academic, New York, 1977).
[46]L. C. Feldman and S. T. Picraux, in *Ion Beam Handbook for Material Analysis,* edited by J. W. Mayer and E. Rimini (Academic, New York, 1977).
[47]R. F. Egerton, Ultramicroscopy 3, 243 (1978).
[48]Prepared by G. Müller-Vogt, University of Karlsruhe.
[49]C. E. Kuyatt and J. A. Simpson, Rev. Sci. Instrum. **38**, 1 (1967); **38**, 103 (1967).
[50]J. Daniels, C. Festenberg, H. Raether, and K. Zeppenfeld, in *Optical Constants of Solids by Electron Spectroscopy,* Vol. 54 of *Springer Tracts in Modern Physics,* edited by G. Höhler (Springer, New York, 1970), p. 77.
[51]F. Wooten, *Optical Properties of Solids* (Academic, New York, 1972).
[52]G. B. Wilson, Proc. Phys. Soc. London 76, 4 (1960).
[53]W. Y. Liang and A. R. Beal, J. Phys. C **9**, 2823 (1976).
[54]J. A. Appelbaum and D. R. Hamann, in *Proceedings of the International Conference on the Physics of Transition Metals, Toronto, 1977,* edited by M. J. G. Lee, J. M. Perz, and E. Fawcett (IOP, London, 1978), p. 111.
[55]G. Lehmann and M. Taut, Phys. Status Solidi **54**, 469 (1972).
[56]J. Pflüger, J. Fink, W. Weber, K.-P. Bohnen, and G. Crecelius (unpublished).